

## Influence of Stenosis Shape, Lesion Length, Eccentricity, and Diameter on Fractional Flow Reserve in Coronary Arteries: A CFD Study

Symon Feolino<sup>1\*</sup>, Murshied Aloyod<sup>2</sup>, Kim Aaron Bravo<sup>3</sup>, Bonifacio Doma<sup>4</sup>

<sup>1</sup>School of Graduate Studies, Mapua University, 658 Muralla St., Manila, 1002, Philippines

\* Corresponding Author Email: [sjfeolino@mymail.mapua.edu.ph](mailto:sjfeolino@mymail.mapua.edu.ph) - ORCID: 0009-0002-9851-8002

<sup>2</sup>Mindanao State University-Lanao del Norte Agricultural College, Sultan Naga Dimaporo, 9223, Philippines

<sup>2</sup>School of Graduate Studies, Mapua University, 658 Muralla St., Manila, 1002, Philippines

Email: [mursh.thermo@gmail.com](mailto:mursh.thermo@gmail.com) - ORCID: 0009-0002-5195-7067

<sup>3</sup>School of Graduate Studies, Mapua University, 658 Muralla St., Manila, 1002, Philippines

Email: [kambravo@mymail.mapua.edu.ph](mailto:kambravo@mymail.mapua.edu.ph) - ORCID: 0009-0008-6922-8317

<sup>4</sup>School of Graduate Studies, Mapua University, 658 Muralla St., Manila, 1002, Philippines

Email: [bt doma@mapua.edu.ph](mailto:bt doma@mapua.edu.ph) - ORCID: 0000-0002-5537-2018

### Article Info:

DOI: 10.22399/ijcesn.1802

Received : 10 February 2025

Accepted : 22 April 2025

### Keywords

Arterial Stenosis,  
Fractional Flow Reserve,  
Stenosis Geometry,  
Lesion Length,  
Computational Modelling

### Abstract:

Arterial stenosis, condition characterized by abnormal narrowing of blood vessels, disrupts blood flow and raises the risk of serious cardiovascular complications. Previous studies indicate highlight that stenosis geometry, lesion length and eccentricity can significantly impact on blood flow characteristics; however, detailed analyses on the combined effects of these parameters remain limited. This study aims to investigate the effects of different stenosis geometries, lengths, and eccentricities on artery's fractional flow reserve (FFR), velocity magnitude and static pressure. Using two stenosis levels (80% and 90%) and two lesion lengths (10 mm and 20 mm), arterial flow across rectangular, elliptical, triangular, and trapezoidal geometries are computationally modelled under both concentric and eccentric configurations. The results show that abrupt shapes, such as triangular and rectangular lesion, create high velocity spikes and pressure gradient near lesion edges, resulting in elevated shear stress. Shear stress and flow disturbance were reduced by smoother shapes, especially elliptical and trapezoidal configurations, which were linked to more gradual velocity and pressure transitions. Additionally, concentric models generally yield higher FFR values, indicating better flow preservation. Rectangular and trapezoidal shapes showed lower FFR values, particularly in eccentric conditions with severe stenosis, while triangular shapes showed relatively high FFR values, suggesting a lower impact on flow.

## 1. Introduction

Cardiovascular diseases (CVDs), including coronary artery disease (CAD), cardiac arrest, and heart failure, remain the leading cause of death globally [1]. Atherosclerosis, in which plaque accumulates on artery walls and causes stenosis, or arterial narrowing, is the main cause of CAD. This process limits blood flow, which results in less oxygen delivery to tissues and, extreme situations, myocardial infarction and ischemia [2].

The Fractional Flow Reserve (FFR) is a critical diagnostic tool in cardiology which assesses the functional severity of coronary arteries stenosis,

helping guide appropriate treatment [3]. It is defined as the ratio of the maximal myocardial blood flow in the presence of stenosis to the theoretical flow without stenosis. Specifically, it is the distal coronary pressure and  $P_a$  is the aortic pressure during maximal hyperemia, and typically it is measured during induced hyperemia using adenosine [4].

According to Mastoi et al. (2018), the conventional FFR measurement is an invasive process that involves using a pressure wire to measure the patient's pressure values [5]. This procedure is expensive for hospitals and poses risks to the patient. A normal result ranges from 0.94 to 1, and any

number below means you need some type of treatment because your blood flow is less than what it should be. For example, values less than or equal to 0.9 indicate a significant likelihood of critical stenosis, having a sensitivity of 92.8 percent and specificity of 82 percent [6]. Patients having FFR of less than 0.8 are classified as high risk because your narrow section of the coronary artery is causing a 20% decrease in pressure [7].

The potential of computational approaches for predicting FFR in coronary arteries has drawn interest. Computational fluid dynamics (CFD), numerical modeling, and image segmentation algorithms could be used to analyze more patient cases and improve their results. The accuracy of CFD-based FFR estimations, however, depends on accurately capturing the physiological features of stenotic lesions, including shape, lesion length, eccentricity, and vessel diameter. These factors influence flow patterns and pressure gradients, which are crucial for precise FFR assessment. Research has shown that lesion geometry significantly alters local hemodynamics, with non-symmetrical shapes, for instance, causing complex recirculation zones that affect FFR readings [8]. Additionally, elongated lesions tend to generate higher pressure drops, while eccentric lesions produce variable flow and pressure distribution, further complicating FFR prediction models [9], [10].

While previous studies have explored individual factors impacting FFR, a comprehensive CFD analysis that simultaneously considers stenosis shape, lesion length, eccentricity, and vessel diameter remains limited. Integrating these factors could improve FFR prediction accuracy, potentially leading to more precise clinical decision-making. This study aims to fill this gap by systematically analyzing the influence of these morphological characteristics on FFR in idealized coronary artery geometries using CFD simulations. By analyzing various stenosis types, including concentric and eccentric lesions, the research aims to provide valuable insights into the physiological interactions between lesion morphology and coronary blood flow, enhancing the potential of CFD as a non-invasive FFR assessment tool.

## 2. Material and Methods

This paper aims to examine how variations in stenosis geometries—specifically shape, lesion length, eccentricity, and diameter—affect the fractional flow reserve (FFR) in coronary arteries. By employing Computational Fluid Dynamics (CFD), the study seeks to simulate blood flow through stenosed arteries, enabling a detailed

analysis of how each geometrical factor influences FFR values. The significance of these relationships is important in determining the degree of the arterial lesions' severity since FFR is a common tool used in assessing the clinical value of coronary artery stenosis. The findings obtained may also facilitate accurate diagnosis and effective management of patients with CAD and expand the role of FFR in practice to a number of clinical scenarios involving varied stenoses.

Clinical studies indicate that stenosis does not typically exhibit a specific shape [11], [12], [13]; however, this study will investigate the geometric influence of stenosis on fractional flow reserve (FFR) by analyzing cases with stenosis areas of 80% (intermediate) and 90% (severe). The data used in this study were based on stenosis dimensions from single lesions in single-vessel pericardial coronary artery disease (CAD) cases, collected from a group of 32 patients, as detailed in Table 1 [14]. A 3D model was then created using the Computer-Aided Design software ANSYS, as shown in Fig. 1. The geometries include rectangular, triangular, elliptical, and trapezoidal shapes, based on those presented in the study by [15]. All dimensions are in millimeters (mm).

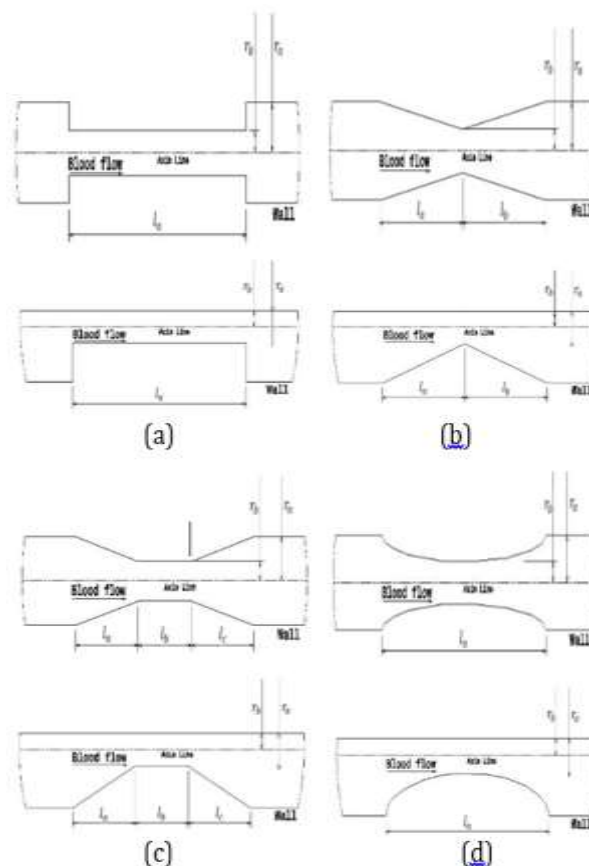


**Figure 1.** Schematic diagram for (a)rectangular, (b)triangular, (c)trapezoidal, and (d)elliptical lesion geometry.

**Table 1.** Dimensions of the Stenosis Model [14]

Area of Stenosis	Lesion Length	$r_a$	$r_b$	Rectangular	Triangular		Trapezoidal			Elliptical
					$l_a$	$l_b$	$l_a$	$l_b$	$l_c$	
80%	10	1.5	0.67	10	5	5	3.5	3	3.5	10
90%	10	1.5	0.47	10	5	5	3.5	3	3.5	10
80%	20	1.5	0.67	20	10	10	7	6	7	20
90%	20	1.5	0.47	20	10	10	7	6	7	20

## 2.1 Modelling

This work regarding blood flow is realized in the study as a non-Newtonian, incompressible, viscous and laminar fluid subject to the Navier-Stokes equations:

$$\rho \left( \frac{\partial u}{\partial t} + u \cdot \nabla u \right) = -\nabla p + \mu \nabla^2 + f \quad (1)$$

where  $\rho$  is the fluid density;  $u$  is the velocity vector;  $t$  is time;  $p$  is pressure;  $\mu$  is the dynamic viscosity; and  $f$  stands for body forces exerted on the fluid.

The continuity equation for incompressible as well as non-compressible particulates is expressed as follows:

$$\nabla \cdot u = 0 \quad (2)$$

The blood stream is in this case treated as an incompressible, non-Newtonian fluid with the help of the Carreau model which defines the model of the viscosity under different shear rates. The Carreau model is given as:

$$\mu = \mu_\infty + (\mu_0 - \mu_\infty) \left( 1 + (\beta \dot{\gamma})^2 \right)^{\frac{n-1}{2}} \quad (3)$$

where  $\mu_0 = 0.056$  kg/ms,  $\mu_\infty = 0.0035$  kg/ms,  $n = 0.3568$ , and  $\beta = 3.313$ s [16].

## 2.2 Boundary and Initial Conditions

A three-dimensional numerical model using ANSYS was used to simulate and study blood flow dynamics in this study. At the outlet of the artery through which the flow is directed, a static pressure boundary condition equal to  $P = 13,332.24$  Pa was introduced, which imitates the physiological state at the distal point of the artery [17]. For the velocity profile to be valid for the inflow conditions, models considering 80% and 90% arterial stenoses (AS) with a mean hyperemic flow rate of  $Q = 165$  mL/min or  $V = 0.389$  m/s and a stated model artery radius of  $r = 1.5$  mm were utilized [18], [19]. These flow profiles tend to be well above normal baselines in large arteries and are the consequence of hyperemia for stenotic arteries. When hyperemic pressure is present, stroke pressure pulses can change the flow on the stenotic lesion because of differences in local structure. This can lead to a number of possible turbulent flow patterns for the three stenosis models of the artery that were studied.

The arterial wall boundary was treated as a rigid wall, and a no-slip velocity boundary condition was applied along the walls. The no slip condition assumes that the wall has a fluid velocity equal to zero, an assumption that is frequently employed to model the way blood flows closer to the arterial wall. Such an arrangement was designed to include the main hemodynamic parameters as well as flow disturbances that stem from stenotic lesions and to explore the aspects of flow separation, recirculation, and shear in stenotic arterial geometry during metabolic stress.

## 2.3 Fractional Flow Reserve

Fractional Flow Reserve (FFR) is calculated using the formula:

$$FFR = \frac{P_d - P_v}{P_a - P_v} \quad (4)$$

where  $P_d$  is the pressure measured at the end of flow reversal occurring distal to the stenosis (mmHg),  $P_a$  is the proximal pressure (mmHg) and  $P_v$  is the venous pressure, which is considered to be 0 mmHg [20].

## 2.4 Numerical Simulation

Numerical simulation of human blood flow in a stenosed artery employs a carefully structured mesh and boundary configuration to ensure accurate representation of hemodynamic behavior. No local sizing is applied, and the surface mesh is generated with a controlled growth rate of 1.05. The geometry consists solely of a fluid region with no voids to maintain simulation integrity. The boundary conditions are defined as follows: a velocity inlet at the inlet and a pressure outlet at the outlet, while the artery walls are assigned as "wall" boundaries. Careful attention is paid to mesh quality so that the minimum orthogonal quality does not go below 0.6 and the maximum skewness is less than 0.5. A 6-layered offset method is employed, starting with an aspect ratio of 12 and a growth rate of 1.05, so as to accurately represent the boundary layer effects. Fluent, acting as the solver, resolves the boundary using a polyhedral mesh, enhancing solution accuracy and maintaining a constant growth ratio of



Figure 2. Computational mesh used for numerical study.

Table 2. Average number of elements for each geometry in the ANSYS Fluent simulation

Geometry	Average Number of Elements
Rectangular	69,598
Triangular	23,251
Trapezoidal	27,092
Elliptical	199,955

1.05 for each layer of the mesh. Table 2 shows the average number of elements for each geometry in the ANSYS Fluent simulation and Figure 2 shows computational mesh used for numerical study.

### 3. Results

Figures 3 and 4 illustrate the variations in velocity magnitude, and Figures 4 and 5 illustrate the variations in static pressure along the artery at different positions during the cardiac cycle. These highlight both eccentric and concentric stenosis models at 80% and 90% area stenosis (AS). The results specifically focused on lesion lengths of 10 mm and 20 mm, revealing the impact of the parameters on the characteristics of arterial flow.

The results, shown in Fig. 3 and Fig. 4, show that the velocity profile always peaks during the systolic phase instead of the diastolic phase for all models and levels of stenosis. The blood velocity shows minimal variations across different geometries in the proximal region. However, the velocity significantly increases as the stenosis percentage increases, with the highest values observed in the 90% AS models. The maximum velocity occurred at the stenosis throat or the mid-stenosis region, with the rectangular shape model producing the highest velocities, followed by the trapezoidal and elliptical shapes. Figures 5 and 6 show the static pressure variations along the artery. When blood comes into contact with the stenosis, the pressure drops, a crucial indicator of the severity of the stenosis, spikes and then gradually decreases. The figures also show that the pressure drop increases as the percentage of area stenosis (AS) increases.

#### 3.1 Velocity Profile

Rectangular configuration models, as shown in Fig. 3a and Fig. 3b, exhibit a relatively high velocity between the edges of a lesion, particularly for shorter lesions measured in the range of 10 mm. This form

causes an abrupt displacement in the flow profile of the blood as it travels across the lesion. The velocity profile shows spikes at the lesion boundaries due to the rectangular shape's rigid transitions. The elliptical model with a short lesion length provides a gradual change in the velocity profile. Due to the model's rounded edges, there's a smoother transition of flow velocities at the boundaries, reducing the intensity of disturbance. This model displays high velocities at the peak of the lesion due to the shape's rapid increase in speed, followed by an equally rapid decline as the flow adapts to the triangular shape. Trapezoidal models with short lesions exhibit moderate changes in entry and exit points, accompanied by relatively stable flow regions on the trapezoid's torso.

The longer length of lesion (20 mm) may result in a mild diffusion of the velocity profile within the central region towards the lower bounds, as indicated in Fig. 3c and Fig. 3d, since enhanced adjustment of fluid flow is aided by an extended lesion. However, with a rectangular geometry, the lesion still has high velocities at its inlet and outlet regions, and hence there are likely to be high fluid stresses with very high shear near the edges of the lesion. Allowing more stabilization of the velocity within the lesion, the elliptical shape can maintain a less rougher velocity profile over the length of the lesion. The model's gradual appearance results in the least disturbance of flow among all models, thereby reducing the likelihood of adverse flow patterns and shear stress along the length of the lesion. We still believe the triangular profile to have a less extreme peak, but the prevalence of angular triangles in the triangular shapes suggests that the velocity will likely remain wide. Longer lesions may exhibit smoother velocity trends after the peak, even though the localized triangular geometry generates high shear stresses. Due to the flatter top of the trapezoidal model, the lesion's length can sustain steady velocity. Such geometries should result in controlled shear stresses and, more importantly, assist in preventing high shear stresses at the edges. The eccentric model exhibits unique variation in the velocity profiles with the geometry and the lesion lengths. Rectangular and triangular-shaped lesions dominate the abrupt velocity change that occurs with a smaller lesion of 10 mm. Lesions that are longer, 20 mm in length, seem to produce a more stable flow pattern, most notably in elliptical and trapezoidal models, which produce smooth transitions and lower shear stress values.

With the shorter lesion length of 10mm in Fig. 4a and Fig. 4b, the concentric model for a rectangular lesion shows a sudden and symmetrical change in velocity at the lesion's edges. Due to the abrupt transitions of the rectangular shape, velocity profiles

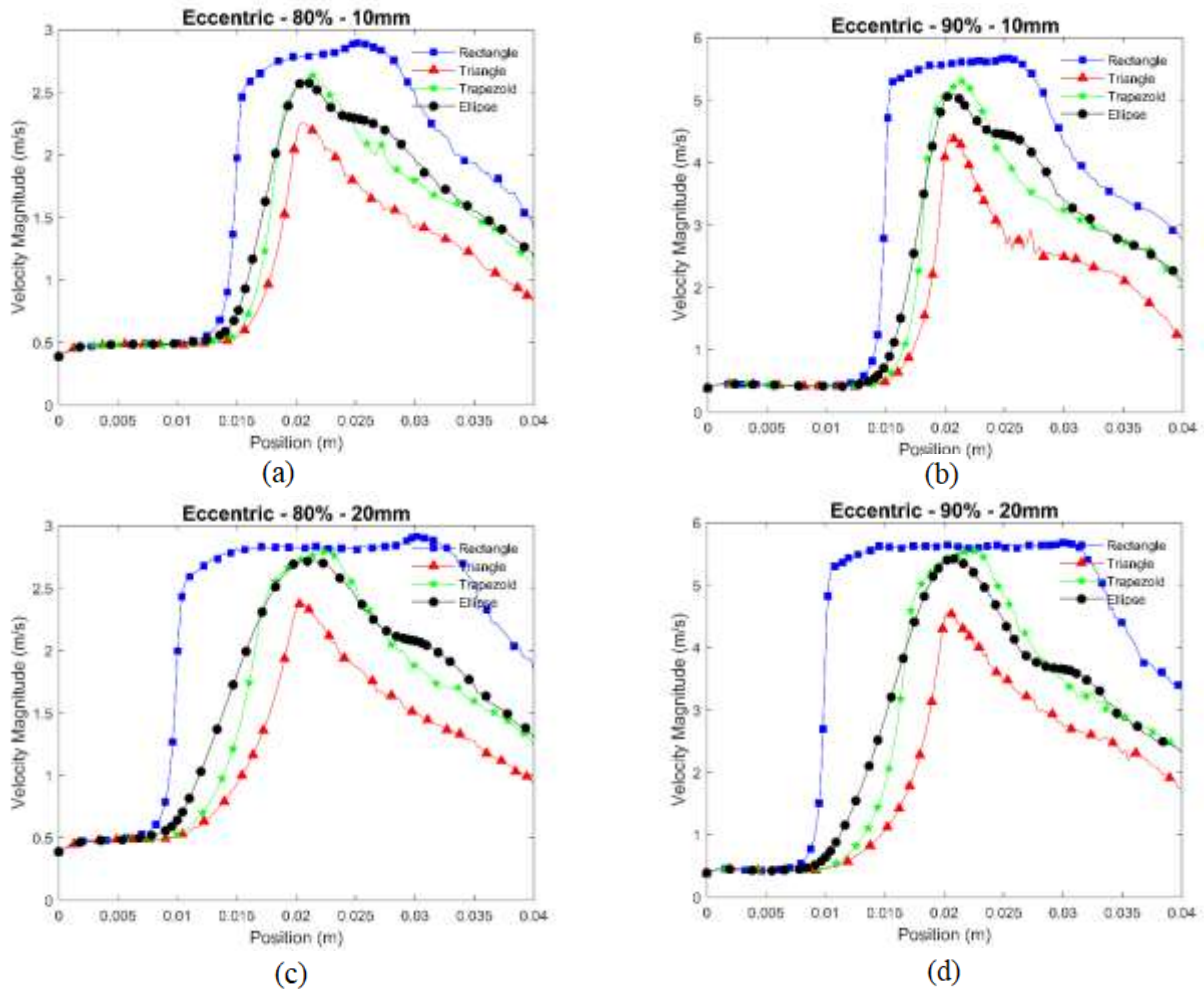


**Figure 3.** Velocity magnitude along the artery at various positions during the cardiac cycle using eccentric model: (a) and (b) 10 mm lesion length, and (c) and (d) 20 mm lesion length

might demonstrate peak values around the edges of the lesion, leading to regions of high shear stress. The concentric positioning ensures that flow is symmetrically distributed, with pronounced variations at the lesion's entry and exit points. The elliptical model with a 10mm lesion length introduces a more gradual velocity change due to the smooth transition at the lesion's boundaries. This orientation, together with a concentric geometry, allows a more even flow, thus decreasing the subsequence of higher velocities at the edges of the lesion area compared to the rectangular model. The concentric cylinder works well with the elliptical shape, providing a more natural flow with low turbulence, while the symmetrical nature of the cylinders makes the flow uniform. The triangular cross-section creates sharp angles that induce high velocity peaks at the apex of the lesion. The length of 10 mm further emphasizes this, as the concentric model provides an even yet narrow peak velocity that fits the shape of the lesion. Such sudden changes may result in the formation of local high velocity zones at the top and increased shear stress around the peak. The trapezoidal shape with a 10mm lesion

length shows a moderate increase in velocity at entry and exit points, with a relatively steady velocity profile over the flat region of the lesion. This profile benefits from the concentric model's symmetry, which provides consistent flow with moderate disturbances only at the edges.

Figures 4c and 4d, which depict a larger lesion length of 20 mm, indicate that the rectangular model velocity profile likely creates a plateau within the lesion, characterized by steep changes in entry and exit velocities due to the geometry. Simply put, the concentric model stabilizes the flow path, but it still causes excessive flow disturbances within the perimeter, thereby confining the lesion area and potentially influencing the shear stress distribution across the artery wall. The elliptical profile allows for even smoother flow across the lesion. The velocity remains more stable throughout the lesion length, with reduced impact at the entry and exit points due to the continuous and rounded shape. Although the overall velocity profile of triangular shapes may be milder and less abrupt, it still includes significant range changes. When you use the concentric model, the area flow along the axis stays

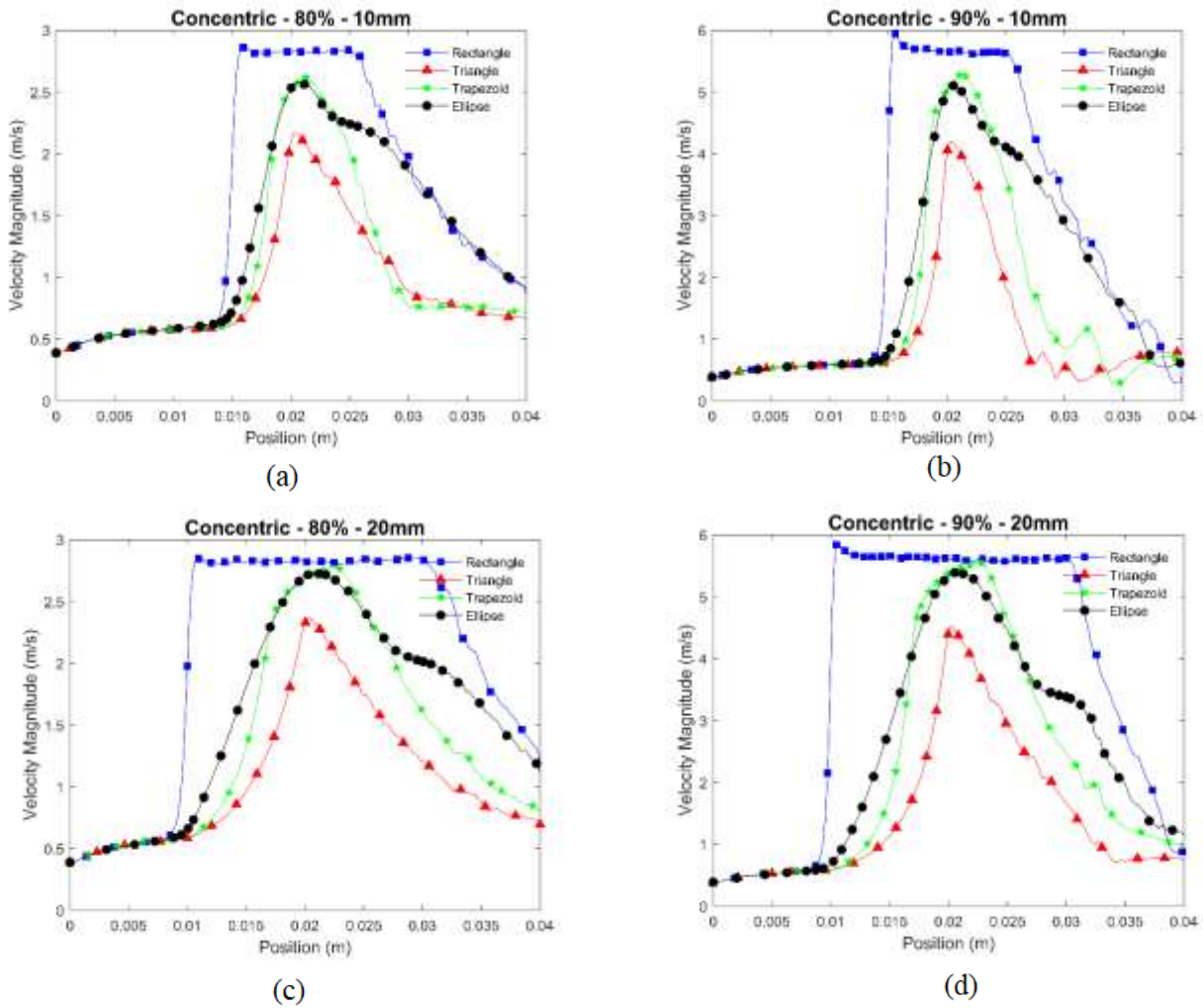


**Figure 4.** Velocity magnitude along the artery at various positions during the cardiac cycle using concentric model: (a) and (b) 10 mm lesion length, and (c) and (d) 20 mm lesion length

the same. But when you use the triangular shape, you get different planes of shear stress over the area. This means that the speeds along the length of the lesion are smoother, but there are two peaks at the ends. When compared to a shorter lesion, the longer length results in a modest decrease in the peak velocities. The trapezoidal model suppresses the velocity profile variations to a greater extent than previously achieved across the lesion's flat surface. Due to its design, the concentric model ensures a smooth and balanced flow path, thereby diminishing the velocity peaks at both the entry and exit points.

The concentric model creates comparable velocity changes within all shapes, even though distinct velocity features are presented with each geometry. For instance, shorter lesions (10 mm) tend to have more pronounced velocity changes, especially in models with abrupt shapes such as rectangular and triangular corners. On the other hand, longer lesions (20 mm) display more steady-state velocity profiles, particularly in the elliptical and trapezoidal lesions, which have lower shear stress and smoother flows.

These results underscore the role of lesion configuration in flow patterns in terms of flow dynamics, which can be important for the vasculature. It has been observed that the concentric model increases stability of the velocity profiles and reduces shear stress in all the lesion shapes, which encourages the use of designs with gradual geometries for the ultimate enhancement of blood flow dynamics.

### 3.2 Pressure Profile

With the 10 mm lesion length in Fig. 5a and Fig. 5b, the rectangular models show a steady pressure drop across the lesion area, indicating a somewhat uniform resistance to blood flow. The elliptical models show a gradual pressure decrease at the 10 mm lesion length. In comparison to the rectangular model, the rounded edges illustrate a less abrupt pressure differential, indicating a smoother flow transition. The triangular model demonstrates a higher pressure gradient immediately adjacent to the

beginning of the lesion and then stabilizes; this is attributable most likely to the narrowing apex shape of the lesion. These steep initial drops signify the larger head-onset resistance, which may lead to increased flow disruption. At lesion length 10 mm, the trapezoidal model portrays a moderate pressure gradient. These additional transformations lead to an increase in opening and closing angles, which will cause a more favorable flow profile.

Figures 5c and 5d clearly demonstrate that the pressure drop across the rectangular lesion intensifies with a lesion length of 20 mm. There appears to be a constant gradient in this case, showing that as the length of the lesion increases, its resistance also increases. Blood passes through an artery, encountering a constant section that narrows with increasing distance, as expected. The elliptical model depicts a moderate pressure drop, though the pressure distribution curve is not as sharp compared to the rectangular profile. This contour shape reduces turbulence and flow disruptions and thus presents a lesional effect that is less disruptive to blood flow. The triangular model also exhibits a persistent pressure drop, albeit with greater stabilization toward the end of the lesion. This shape increases the dimensionality of the lesion length, which in turn expands the effect of initial resistance, resulting in a more complex gradient throughout the artery. For the trapezoidal model, a consistent gradient can be observed, which only increases slightly in magnitude for the lesion of seven millimeters in length. A comparison of figures shows that a trapezoidal shape is effective in mitigating pressure loss compared to triangular and rectangular shapes due to its moderate curve slope. This further suggests that the trapezoidal model would cause less disruption in flow, even when the length of the lesions increases.

The pressure profiles suggest that for all the models, the pressure drop increases with the elongation of the lesion. The rectangular and triangular models result in greater changes in pressure, indicating higher flow resistances. Elliptical and trapezoidal models produce variations in pressure that are less pronounced, hence less disturbance to blood flow. These profiles bring out how the shape and length of the lesions further dictate the pressure dynamics in the arteries, which are very important in understanding flow resistance and effects in arterial stenosis.

Figures 6a and 6b, which show a shorter lesion length of 10 mm, exhibit abrupt edges, leading to a sudden drop in blood pressure as blood passes over the lesion. Such abrupt changes in geometry may further create localized high-pressure regions at the entry and exit points of the lesion, which are bound to create pressure gradients that might interfere with

the flow. The elliptical model, on the other hand, achieves a better pressure distribution throughout the length of the lesion. Because of its round contour, the pressure profile is not as high at the entry and exit of the lesion, which reduces rapid changes in the gradients. The concentric model uses a symmetrical flow path, which results in a gradual loss of pressure and a decrease in localized high-pressure areas. A pressure peak is created at the triangular model, the highest point of the lesion, where blood flow is the most restricted. The existence of this peak produces large pressure differentials across shorter lengths of the lesion as blood moves to and from these constricted areas. In the trapezoidal model, the pressure distribution at both the inflow and outflow ends of the lesion is rather moderate, but over the flat top of the lesion, the distribution is more consistent. The same symmetry characteristic of the concentric model also increases the strength of the pressure profile, providing for greater average stability.

In Figures 6c and 6d, the rectangular model exhibits a larger 20-mm lesion, characterized by a larger area of high pressure at the beginning of the lesion, followed by a decrease in pressure along the lesion's length. Distribution consistency is maintained in the concentric model, but longer lesions may cause a greater total resistance, which may elevate the pressure in and prior to the lesion. The elliptical shape additionally assists in pressure profile stability by ensuring gradual decreases across the lesion with very few peaks. The gradual geometry helps to avoid any abrupt changes in pressure and keeps the profile smooth, hence reducing high shear stress at the edges of the boundaries. For a longer lesion, the pressure profile may be somewhat less abrupt, but the triangular model still shows a pressure increase at the lesion's peak due to the converging walls. The concentric model ensures symmetry in the distribution, but the overall pressure profile remains irregular due to the triangular shape. The trapezoidal model further stabilizes the pressure profile across the lesion. The flat top allows for sustained, stable pressure along the length of the lesion, with minor increases at the entry and exit points.

The concentric model influences the pressure profile by providing a symmetric and balanced flow path. However, each shape's geometry creates unique pressure characteristics. Shorter lesions (10mm) tend to have sharper pressure gradients, particularly in models with abrupt changes (rectangular and triangular). Lesions larger in size (20mm) are found to be more consistent in their pressure profiles, particularly in the elliptical and trapezoidal models, as these shapes help in minimizing pressure spikes. The concentric model could prove to be the most advantageous biomechanical configuration as it utilizes the elliptical and trapezoidal models, which

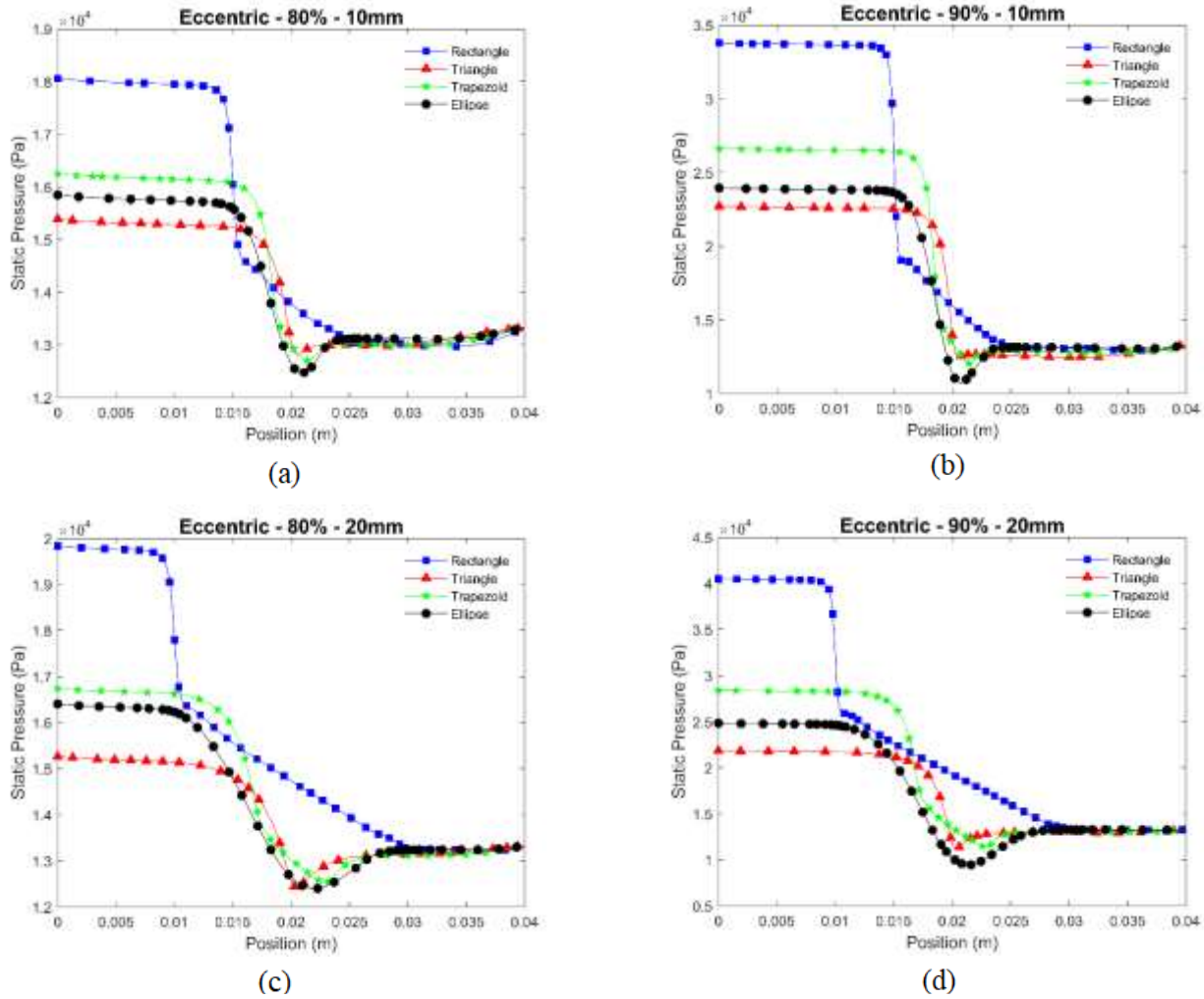


**Figure 5.** Static pressure along the artery at various positions during the cardiac cycle using eccentric model: (a) and (b) 10 mm lesion length, and (c) and (d) 20 mm lesion length.

allow for gradual pressure transitions and lower shear stresses, which can also be beneficial for vascular tubing. The rectangular and triangular models, even if symmetrical, cause a higher pressure gradient and therefore may contribute to higher stress on the arterial walls.

### 3.3 Fractional Flow Reserve

Rectangular geometry in Fig. 7a, whether concentric or eccentric, shows a trend of decreasing FFR with increasing area of stenosis. The concentric model exhibits a slightly higher FFR compared to the eccentric model, indicating that the eccentric positioning results in more flow disturbance and a lower FFR. The elliptical geometry is noted to cause a more gradual decrease in the FFR as compared to the rectangular model. Both the eccentric and concentric models exhibit higher FFR values than the rectangular model, suggesting a reduction in blood flow resistance. The eccentric model experiences lower FFR as well, but this has a higher

area of stenosis. However, this has less effect. Trapezoidal model does not seem to vary as much with increasing stenosis areas. The FFR in the concentric model tends to decrease slowly, while the rates in the eccentric model sharply increase. This suggests that the trapezoidal shape exhibits less violent flow compared to the concentric form. Among these shapes, the triangular model performs the worst, exhibiting a steep decline in FFR and an increase in stenosis in both models, with the eccentric configuration being the most severe. This indicates that the triangular shape's increase in stenosis area leads to an increase in position, which in turn causes great resistance and, consequently, lower FFR values.

With a longer lesion, the rectangular shape in Fig. 7b shows a steeper or sharper drop in the FFR in line with the increase in stenosis, which is more pronounced in the eccentric model. The FFR decreases more pronouncedly in this case compared to the 10 mm lesion, indicating a greater resistance

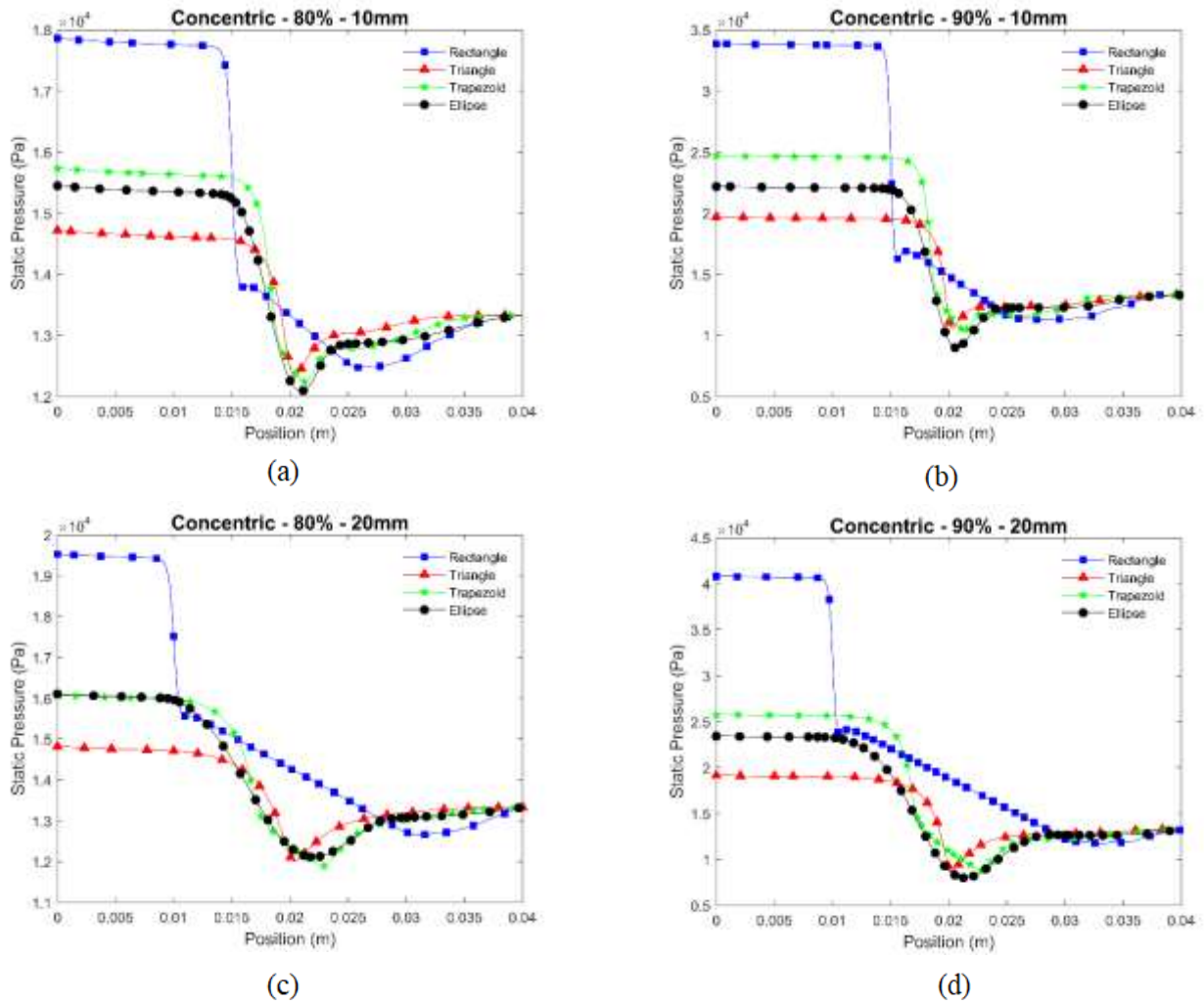


Figure 6. Static pressure along the artery at various positions during the cardiac cycle using concentric model: (a) and (b) 10 mm lesion length, and (c) and (d) 20 mm lesion length.

to the more extensive lesion. The elliptical shape continues to exhibit a smoother FFR decrease than the rectangular and triangular shapes. The concentric

model maintains relatively stable FFR values, while the eccentric model shows a more gradual decline, indicating that the elliptical shape is less affected by

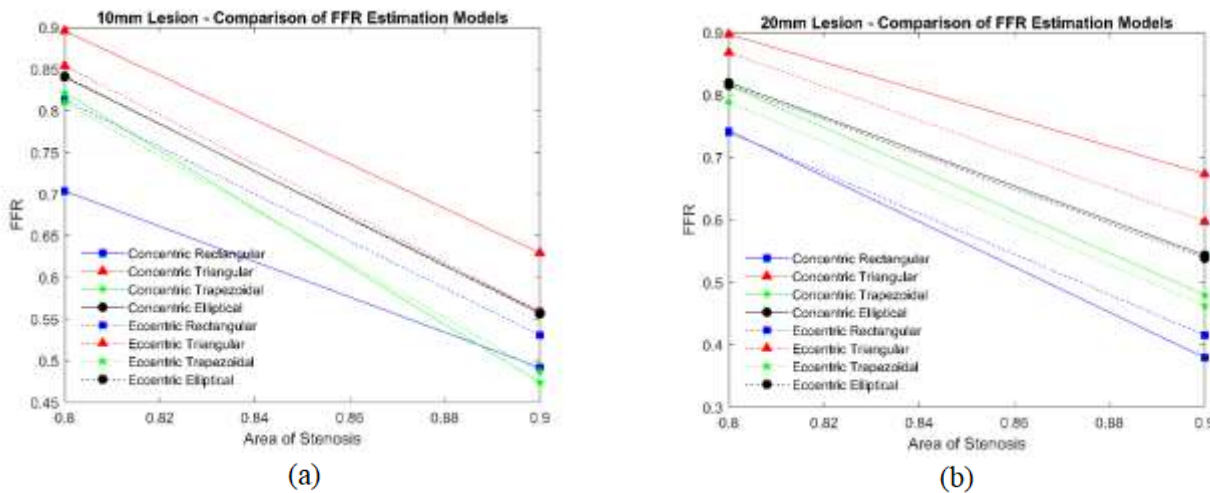


Figure 7. FFR values against Area of Stenosis of the four geometries: Rectangular, Trapezoidal, Elliptical and Triangular in concentric and eccentric models of (a) 10mm lesion, and (b) 20mm lesion.

lesion length. Similar to the 10 mm lesion, the trapezoidal shape maintains higher FFR values in the concentric model but experiences a more rapid FFR reduction in the eccentric model as stenosis increases. This shape remains less disruptive in the concentric setup even with an extended lesion length. For the 20 mm lesion, the triangular shape again demonstrates the steepest FFR decrease across all geometries. Both models, especially the eccentric one, show a significant FFR reduction as stenosis area grows, underlining the triangular shape's increased resistance with greater lesion length.

#### 4. Conclusion

This study demonstrates the significant impact of stenosis geometry, lesion length, and eccentricity on arterial flow characteristics, including velocity profiles, static pressure, and fractional flow reserve (FFR). The analysis emphasizes how the symmetry and form of stenoses are crucial to the dynamics of blood flow in the artery. Sharper velocity and pressure gradients are caused by the abrupt transitions of triangular and rectangular lesions, leading to high shear stress at lesion boundaries. This is particularly noticeable in shorter lesions where there is more evident flow disruption. On the other hand, particularly in concentric configuration, the elliptical and trapezoidal geometries result in smoother velocity and pressure transitions. This reduces the shear stress along lesion boundaries and reduces adverse flow pattern.

In terms of FFR, concentric models generally maintain higher FFR values than eccentric model, this suggests better flow preservation. Triangular stenosis models, out of all the geometries examined, exhibit relatively higher FFR values, suggesting less flow impact, specifically in longer lesions. On the other hand, trapezoidal and rectangular shapes show lower FFR values, particularly at higher stenosis levels (90% AS), indicating more flow impairment under eccentric conditions.

These results highlight the importance of considering lesion geometry and eccentricity when evaluating arterial stenosis because these parameters have a major impact on the degree of flow restriction. In order to increase the diagnostic accuracy for patient specific arterial conditions, this study suggests that the FFR should consider both the shape and orientation of stenosis when performing clinical assessments.

#### Author Statements:

- **Ethical approval:** The conducted research is not related to either human or animal use.

- **Conflict of interest:** The authors declare that they have no known competing financial interests or personal relationships that could have appeared to influence the work reported in this paper
- **Acknowledgement:** The authors declare that they have nobody or no-company to acknowledge.
- **Author contributions:** The authors declare that they have equal right on this paper.
- **Funding information:** The authors declare that there is no funding to be acknowledged.
- **Data availability statement:** The data that support the findings of this study are available on request from the corresponding author. The data are not publicly available due to privacy or ethical restrictions.

#### References

- [1] McDermott, M. M., Kramer, C. M., Tian, L., Carr, J., Guralnik, J. M., Polonsky, T., Carroll, T., Kibbe, M., Criqui, M. H., Ferrucci, L., Zhao, L., Hippe, D. S., Wilkins, J., Xu, D., Liao, Y., McCarthy, W., & Yuan, C. (2016b). Plaque composition in the proximal superficial femoral artery and peripheral artery disease events. *JACC. Cardiovascular Imaging*, 10(9), 1003–1012. <https://doi.org/10.1016/j.jcmg.2016.08.012>
- [2] Khan, F. R., Ali, J., Ullah, R., Hassan, Z., Khattak, S., Lakhta, G., & Gul, N. (2021b). Relationship between high glycated hemoglobin and severity of coronary artery disease in type II diabetic patients hospitalized with acute coronary syndrome. *Cureus*. <https://doi.org/10.7759/cureus.13734>
- [3] Chahour, K. (2019). Modeling coronary blood flow using a non newtonian fluid model: fractional flow reserve estimation. <https://hal.inria.fr/tel-02430901>
- [4] Ciccarelli, G., Renon, F., Bianchi, R., Tartaglione, D., Bigazzi, M. C., Loffredo, F., Golino, P., & Cimmino, G. (2021). Asymptomatic stroke in the setting of percutaneous Non-Coronary intervention procedures. *Medicina*, 58(1), 45. <https://doi.org/10.3390/medicina58010045>
- [5] Mastoi, Q., Wah, T. Y., Raj, R. G., & Iqbal, U. (2018). Automated Diagnosis of Coronary Artery Disease: A review and Workflow. *Cardiology Research and Practice*, 2018, 1–9. <https://doi.org/10.1155/2018/2016282>
- [6] Zengin, I., & Karakus, A. (2023). The importance of baseline fractional flow reserve to detect significant coronary artery stenosis in different patient populations. *Cardiovascular Journal of South Africa*, 34(4), 56–63. <https://doi.org/10.5830/cvja-2023-045>
- [7] Pirković, M. S., Pavić, O., Filipović, F., Saveljić, I., Geroski, T., Exarchos, T., & Filipović, N. (2023). Fractional Flow Reserve-Based patient risk classification. *Diagnostics*, 13(21), 3349. <https://doi.org/10.3390/diagnostics13213349>
- [8] Papafaklis, M. I., Muramatsu, T., Ishibashi, Y., Lakkas, L. S., Nakatani, S., Bourantas, C. V., Ligthart,

- J., Onuma, Y., Echavarría-Pinto, M., Tsirka, G., Kotsia, A., Nikas, D. N., Mogabgab, O., Van Geuns, R., Naka, K. K., Fotiadis, D. I., Brilakis, E. S., Garcia-Garcia, H. M., Escaned, J., . . . Serruys, P. W. (2014). Fast virtual functional assessment of intermediate coronary lesions using routine angiographic data and blood flow simulation in humans: comparison with pressure wire – fractional flow reserve. *EuroIntervention*, 10(5), 574–583. [https://doi.org/10.4244/eijy14m07\\_01](https://doi.org/10.4244/eijy14m07_01)
- [9] Tu, S., Barbato, E., Kőszegi, Z., Yang, J., Sun, Z., Holm, N. R., Tar, B., Li, Y., Rusinaru, D., Wijns, W., & Reiber, J. H. C. (2014). Fractional flow reserve calculation from 3-Dimensional quantitative coronary angiography and TIMI frame count. *КАРДИОЛОГИЯ УЗБЕКИСТАНА*, 7(7), 768–777. <https://doi.org/10.1016/j.jcin.2014.03.004>
- [10] Morris, J. R., Bellolio, M. F., Sangaralingham, L. R., Schilz, S. R., Shah, N. D., Goyal, D. G., Bell, M. R., Kopecky, S. L., Gilani, W. I., & Hess, E. P. (2016). Comparative trends and downstream outcomes of coronary computed tomography angiography and cardiac stress testing in emergency department patients with chest pain: An Administrative Claims analysis. *Academic Emergency Medicine*, 23(9), 1022–1030. <https://doi.org/10.1111/acem.13005>
- [11] Berglund, H., Luo, H., Nishioka, T., Fishbein, M. C., Eigler, N. L., Tabak, S. W., & Siegel, R. J. (1997c). Highly localized arterial remodeling in patients with coronary atherosclerosis. *Circulation*, 96(5), 1470–1476. <https://doi.org/10.1161/01.cir.96.5.1470>
- [12] Tang, D., Yang, C., Kobayashi, S., Zheng, J., & Vito, R. P. (2003c). Effect of stenosis asymmetry on blood flow and artery compression: A Three-Dimensional Fluid-Structure Interaction model. *Annals of Biomedical Engineering*, 31(10), 1182–1193. <https://doi.org/10.1114/1.1615577>
- [13] Moser, K. W., Kutter, E. C., Georgiadis, J. G., Buckius, R. O., Morris, H. D., & Torczynski, J. R. (2000b). Velocity measurements of flow through a step stenosis using Magnetic Resonance Imaging. *Experiments in Fluids*, 29(5), 438–447. <https://doi.org/10.1007/s003480000110>
- [14] Wilson, R. F., Johnson, M. R., Marcus, M. L., Aylward, P. E., Skorton, D. J., Collins, S., & White, C. W. (1988f). The effect of coronary angioplasty on coronary flow reserve. *Circulation*, 77(4), 873–885. <https://doi.org/10.1161/01.cir.77.4.873>
- [15] Sarfaraz, K. (2016). Computational hemodynamic analysis of stenosed coronary artery *Sarfaraz Kamangar*. <http://studentsrepo.um.edu.my/6790/>
- [16] Cho, Z. H., Mun, C. W., & Friedenber, R. M. (1991). NMR angiography of coronary vessels with 2- D planar image scanning. *Magnetic Resonance in Medicine*, 20(1), 134–143. <https://doi.org/10.1002/mrm.1910200114>
- [17] He, X., Lu, Y., Saha, N., Yang, H., & Heng, C. (2005). Acyl-CoA: cholesterol acyltransferase-2 gene polymorphisms and their association with plasma lipids and coronary artery disease risks. *Human Genetics*, 118(3–4), 393–403. <https://doi.org/10.1007/s00439-005-0055-3>
- [18] Konala, B. C., Das, A., & Banerjee, R. K. (2011b). Influence of arterial wall-stenosis compliance on the coronary diagnostic parameters. *Journal of Biomechanics*, 44(5), 842–847. <https://doi.org/10.1016/j.jbiomech.2010.12.011>
- [19] Rajabi-Jaghargh, E., Kolli, K. K., Back, L. H., & Banerjee, R. K. (2011b). Effect of guidewire on contribution of loss due to momentum change and viscous loss to the translational pressure drop across coronary artery stenosis: An analytical approach. *BioMedical Engineering OnLine*, 10(1). <https://doi.org/10.1186/1475-925x-10-51>
- [20] Pijls, N. H. J., Van Gelder, B., Van der Voort, P., Peels, K., Bracke, F. A. L. E., Bonnier, H. J. R. M., & El, M. I. H. (1996). Fractional flow reserve: A useful index to evaluate the influence of an epicardial coronary stenosis on myocardial blood flow. *Circulation*, 93(9), 1806–1813. <https://doi.org/10.1161/01.CIR.93.9.1806>